Combined Arrhenius-Merz Law Describing Domain Relaxation in Type-II Multiferroics

J. Stein,[1] S. Biesenkamp,[1] T. Cronert,[1,*] T. Fröhlich,[1] J. Leist,[2] K. Schmalzl,[3] A. C. Komarek,[1,4] and M. Braden[1,†]
[1]II. Physikalisches Institut, Universität zu Köln, Zülpicher Straße 77, D-50937 Köln, Germany
[2]Institut für Physikalische Chemie, Georg-August-Universität Göttingen, Tammannstraße 6, 37077 Göttingen, Germany
[3]Juelich Centre for Neutron Science JCNS, Forschungszentrum Juelich GmbH, Outstation at ILL, 38042 Grenoble, France
[4]Max Planck Institute for Chemical Physics of Solids, Nöthnitzer Straße 40, D-01187 Dresden, Germany

(Received 20 November 2020; accepted 22 July 2021; published 24 August 2021)

Electric fields were applied to multiferroic $TbMnO_3$ single crystals to control the chiral domains, and the domain relaxation was studied over 8 decades in time by means of polarized neutron scattering. A surprisingly simple combination of an activation law and the Merz law describes the relaxation times in a wide range of electric field and temperature with just two parameters, an activation-field constant and a characteristic time representing the fastest possible inversion. Over the large part of field and temperature values corresponding to almost 6 orders of magnitude in time, multiferroic domain inversion is thus dominated by a single process, the domain wall motion. Only when approaching the multiferroic transition other mechanisms yield an accelerated inversion.

DOI: 10.1103/PhysRevLett.127.097601

The control and inversion of ferroic domains is widely used in numerous technologies. Ferromagnetic domain dynamics have been intensively studied forming the basis of magnetic data storage [1,2]. In contrast ferroelectric domains remain less understood, as the underlying physical processes are more complex [3]. Concerning antiferromagnetic domains, almost no information exists, because there is no driving field available and because visualization can be realized only in special cases [4–7]. Multiferroic phases arise from the coupling of two ferroic order parameters and mostly refer to systems with coexisting magnetic and ferroelectric order [8–10]. In a type-II multiferroic the magnetic structure directly induces ferroelectric polarization. Therefore, an electric field can control magnetic order, which opens new perspectives to study the dynamics of antiferromagnetic domains.

In many type-II multiferroics the sign of the ferroelectric polarization corresponds to the vector chirality of the spins [11,12], which can be measured by polarized neutron diffraction. Therefore, the distribution of magnetic domains can be studied in multiferroics, and such experiments demonstrated the poling of multiferroic magnetism by cooling in electric field [13–15] as well as the domain inversion at constant temperature [14,16,17].

The inversion and relaxation of ferroelectric domains in response to an external electric field was studied on various ferroelectrics [3]. Merz [18] reported for $BaTiO_3$ that the electric-field dependence of the characteristic relaxation time τ follows a simple law $\tau \propto \exp[\alpha(T)/E]$, which is now called Merz law with $\alpha(T)$ being the temperature dependent activation field. The modeling of ferroelectric domain kinetics was further developed by Ishibashi and Takagi [19,20] basing on the Avrami model [21–23] for the kinetics of phase change. These models consider germ nuclei, which develop either continuously or are latent, and the growth of domains in different dimensionality. For a field-induced switching in the case of latent nuclei, the fraction of switched volume $R(t)$ evolves exponentially $R(t) = 1 - \exp\{-[(t - t_0)/\tau]^b\}$. Here t_0 corrects for the latent nuclei density that can be neglected in many cases, and b describes the dimensionality of the growth process. Studies of the temperature and electric-field dependence of the relaxation time in different ferroelectrics, however, did not reveal a common picture. Hayashi [24] and Lines and Glass [25] proposed that the activation field is given by the third power of the electric polarization divided by temperature, $\alpha(T) \propto P_S^3/T$. Assuming a simple temperature dependency of the electric polarization, as it follows for example in Landau theory, one can deduce scaling laws for the relaxation time, which becomes a function of just the quotient of the field and a power of the reduced temperature, $\tau = f(E/T_r^m)$ with $T_r = (T_C - T)/T_C$, but different types of scaling were reported [26,27].

The switching of ferroelectric order consists of different processes [3], which may explain the difficulties to find a simple law for the ferroelectric relaxation times. For the inversion of a ferroelectric thin film Scott resumes three steps [3]: The nucleation at the surface, the forward growth across the film and the sideways growth of the first needle-shaped domains to fully revert the material. If these processes occur on comparable timescales, one may not expect a simple law for the relaxation times resulting from all processes. The inversion of multiferroic domains was studied by optical methods on $MnWO_4$ [28] and on $TbMnO_3$ [29]. These studies reveal a small number of rather large domains, which furthermore mostly extend

along the ferroelectric polarization. This indicates that the sideways growth processes perpendicular to the ferroelectric polarization dominate the inversion of multiferroic domains.

Here we use polarized neutron diffraction under large external electric fields to study the multiferroic relaxation times in the prototype multiferroic $TbMnO_3$ [30]. Polarized neutron diffraction allows one in particular to study the slow relaxation processes because there is no contamination of the chiral signal. We find an astonishingly simple relation for the temperature and electric-field dependence of the relaxation that is described by the combination of Arrhenius and Merz laws. Domain wall motion can be identified as the determining process for switching multiferroic domains over a large range of temperature and electric-field values.

Single crystals of $TbMnO_3$ were grown by the floating zone technique in an image furnace [17] and were characterized by magnetic measurements using a SQUID magnetometer confirming the Néel and multiferroic transition temperatures, ($T_N = 42$ K, $T_{MF} = 27.6$ K) [17].

Polarized neutron diffraction experiments were performed on the IN12 cold triple-axis spectrometer at the ILL [31]. Incoming neutrons were polarized by a cavity placed in the neutron guide yielding an average incoming polarization of 0.94 in the considered wavelength range [31]. As monochromator we used the (0 0 2) reflection of highly oriented pyrolytic graphite (HOPG) and higher order contaminations were suppressed by a velocity selector. Since the analysis of the chiral domains does not require full polarization analysis, we used a nonpolarizing HOPG (0 0 2) analyzer to improve statistics.

Thin plates with thicknesses of $d = 0.9$, 1.32, and 1.61 mm (labeled as samples *SI*, *SII*, and *SIII*, respectively) were cut perpendicular to the ferroelectric polarization (along the c direction) and the electric field was applied by a capacitor of aluminum plates. Further experimental information is given in the Supplemental Material [32].

For neutron polarization parallel or antiparallel to the scattering vector, $\boldsymbol{Q}$, all magnetic scattering results in a neutron spin flip and in the absence of nuclear scattering the intensity is given by $I^{\pm} = \boldsymbol{M}_{\perp}^{*} \cdot \boldsymbol{M}_{\perp} \pm i(\boldsymbol{M}_{\perp}^{*} \times \boldsymbol{M}_{\perp})_x$ [33]. Here $\boldsymbol{M}_{\perp}$ is the Fourier component of the magnetization distribution perpendicular to $\boldsymbol{Q}$ and $()_x$ refers to the component parallel to $\boldsymbol{Q}$. For a perfect chiral system (with the scattering vector perpendicular to the plane of the magnetic moments), for which $\boldsymbol{M}_{\perp}^{*} \cdot \boldsymbol{M}_{\perp}$ and $(\boldsymbol{M}_{\perp}^{*} \times \boldsymbol{M}_{\perp})_x$ are of the same size, the total magnetic scattering appears in one of these two intensities, I^{+} or I^{-}, while the other one vanishes. $TbMnO_3$ exhibits a nearly perfect chiral structure and the scattering vector, $\boldsymbol{Q} = (2, 0.28, 1)$, was chosen nearly perpendicular to the cycloid plane, so that the chiral ratio, $r_{\text{chiral}} = (I^{+} - I^{-})/(I^{+} + I^{-})$, nearly corresponds to the domain distributions with positive or negative electric polarization [17]. By recording the chiral ratio during the domain inversion we thus directly determine the ratio of the chiral and multiferroic domains.

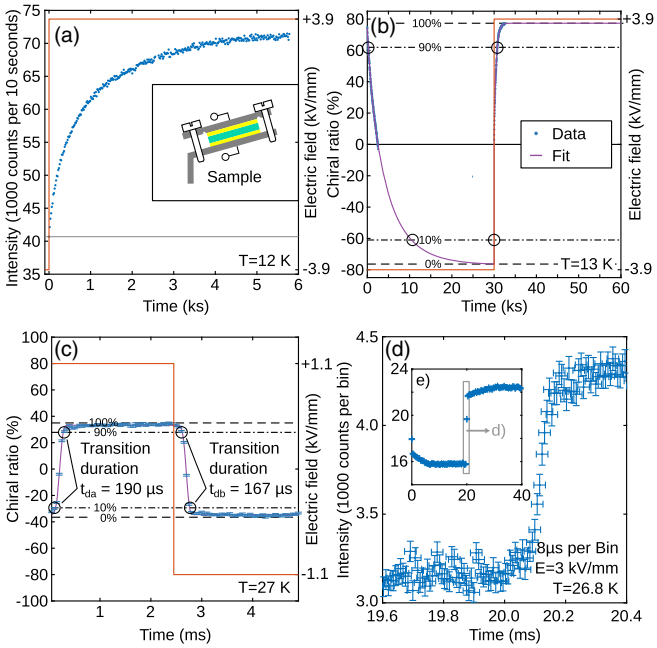

FIG. 1. Panels (a) and (b) show very slow inversion of multiferroic domains in $TbMnO_3$ observed at low temperatures, where several hours are needed to invert domains. In contrast, the panels (c) and (d) show the fastest switching of chiral magnetism that could be observed at high fields close to the long-range multiferroic transition temperature (in zero field). Red lines indicate the electric field. Data in panels (a)–(c) and in (d) was taken with crystal *SI* and *SII*, respectively. Dashed-dotted horizontal lines indicate the 10% and 90% values of domain inversion and dashed lines 0% and 100%.

The time dependence of r_{chiral} and thus of the domain distribution is fitted by an exponential relaxation:

$$r_{\text{chiral}}(t) = r_a - (r_a - r_b)\exp\left[-\left(\frac{t}{\tau_a}\right)^b\right], \quad (1)$$

$$r_{\text{chiral}}(t) = r_b - (r_b - r_a)\exp\left[-\left(\frac{t - t_{1/2}}{\tau_b}\right)^b\right], \quad (2)$$

in the first half-period, Eq. (1), when switching from r_b to r_a and when switching back, Eq. (2) (with relaxation constant τ_b), respectively; $t_{1/2}$ denotes half of the period. Alternatively, one may define a transition duration t_d as the time between 10% and 90% of the switching process, see Fig. S1 in the Supplemental Material [32]. For the faster processes we use a stroboscopic setup [34] described in the Supplemental Material [32]. The direction of the electric field alternates periodically, while we record the neutron signal with a time stamp in respect of the electric field inversion.

The wide span of timescales that can be studied by polarized neutron diffraction is illustrated in Fig. 1. For the

lowest two temperatures studied, the relaxation becomes very slow and hours are required to invert the domains. A considerable asymmetry points to a preference of the system for a direction of electric polarization combined with a preferred chirality [14]. For these measurements the stroboscopic technique [34] is not needed, but simple counting as a function of time is sufficient. These extremely slow neutron experiments are possible, because the application of the electric field has no further impact on the chiral signal. This is in contrast to dielectric measurements where electric relaxation other than that of the multiferroic domains can be very strong [35].

The most rapid switching of chiral magnetism occurs at high temperatures and large electric fields. In a measurement using the stroboscopic setup at 27 K and 1.1 kV/mm we observe transition durations of 190 and 167 μs, and even faster processes were observed at 26.8 K and 3 kV/mm with a transition duration of the order of 50 μs, see Figs. 1(c) and 1(d). These switching rates reach the intrinsic limitations of time-resolved neutron diffraction on IN12 of about 50 μs resulting essentially from the finite wavelength spread and the variation of flight lengths due to the finite dimensions of the sample, diaphragms, and detector. Furthermore, the dielectric loss of the rapidly switching electric field implies power dissipation in the sample that heats the sample and cannot be neglected anymore. With the higher voltage the crystal is probably heated above the long-range multiferroic transition temperature, where chiral switching nevertheless persists [17]. In a functional device one will also deal with small multiferroic regions that apparently can be more rapidly controlled than the bulk crystal deep in the multiferroic phase. Summarizing, polarized neutron diffraction can study multiferroic relaxation processes over about 8 decades in time [36].

In Fig. 2 we show typical switching curves fitted by exponential relaxation, Eqs. (1) and (2), from which we get the exponents b and the relaxation times, τ_a and τ_b, for the two field-sweep directions. One notices the wide span of relaxation times that appear as a function of temperature, while the shape of the switching curves does not essentially change. This is further illustrated in Fig. 3(a), showing switching curves normalized by the relaxation times and by the maximum chiral ratio, which correspond well with each other in this scaling. The stretching exponents are plotted in Fig. 3(b) and vary little at temperatures more than 1 K below T_{MF}. However, close to the transition the exponents considerably increase. In the formalism of the Ishibashi theory, the exponent can be associated with the dimensionality of the germ growth. The growth is between one- and two-dimensional and the exponent increases close to T_{MF}, when the nucleation process can become continuous [19,20].

The relaxation times for the two directions of field switching are shown in Fig. 4(a) in a logarithmic plot against the inverse temperature. In the logarithmic plot the slight differences between the two directions are irrelevant.

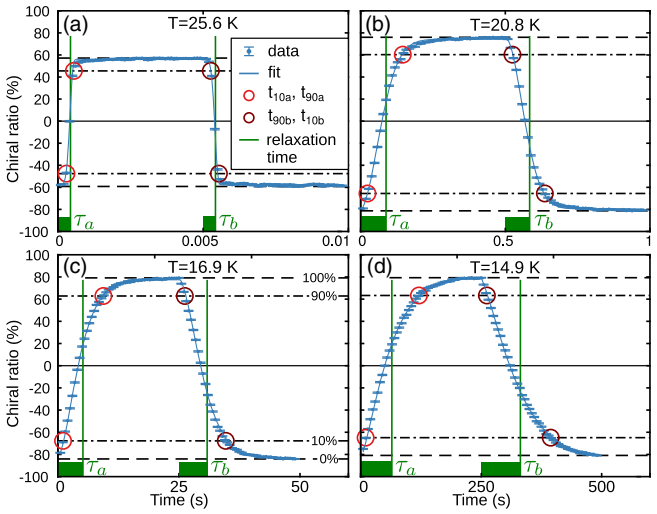

FIG. 2. Typical switching curves observed for $TbMnO_3$ with an electric field of 3.9 kV/mm at various temperatures. Lines denote the fitted exponential relaxation [Eqs.(1) and (2)] to extract the relaxation times for both directions of field change thereby defining the relaxation time τ_a,τ_b indicated by green bars and vertical lines. Dashed-dotted horizontal lines indicate the 10% and 90% values of domain inversion and dashed lines 0% and 100% (data taken with sample *SI*).

At each field the data can be very well fitted by a linear activation (Arrhenius) behavior, $\tau \propto \exp(A'/T)$, see Fig. S2 in the Supplemental Material [32]. Just close to the multiferroic transition the relaxation is faster than extrapolated from the activation law. For the largest field this activation behavior is observed over 6 decades in time while the

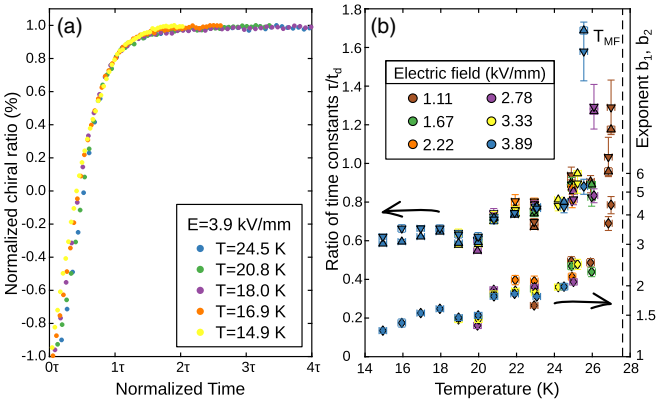

FIG. 3. (a) The switching curves obtained for $TbMnO_3$ with an electric field of 3.9 kV/mm at various temperatures are normalized to the relaxation times and to the maximum chiral ratio thereby confirming the qualitatively identical shape. (b) The stretching exponents b of the relaxation for both directions are plotted against the temperature. The color coding distinguishes different values of the electric field and the triangles denote the direction of the field change. Except close to the transition, the exponents vary little. The ratio between duration and relaxation times resulting from these exponents is also shown in panel (b). All data taken on sample *SI*.

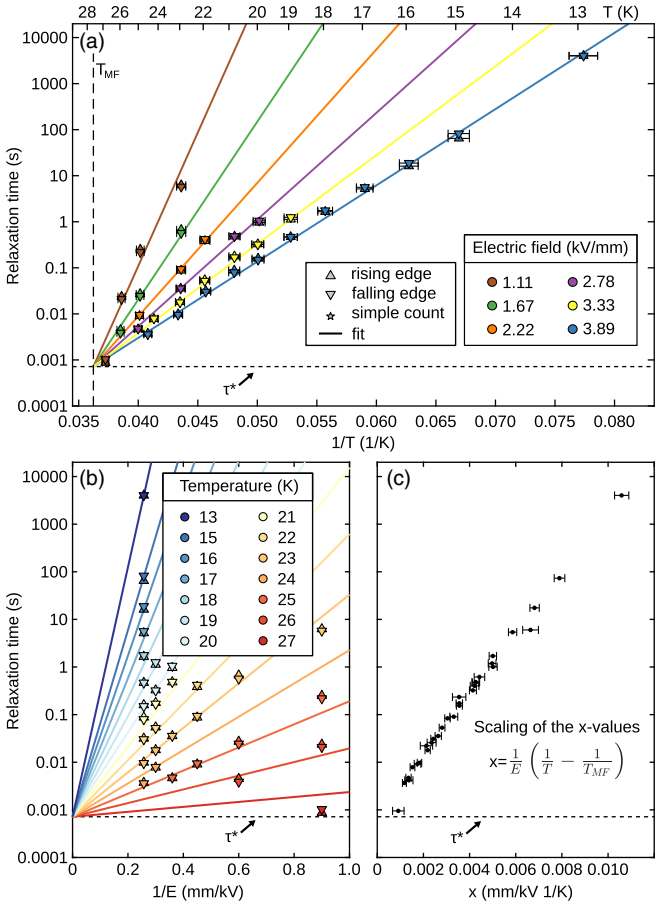

FIG. 4. (a) Logarithmic plot of the relaxation times as a function of the inverse temperature for the two switching directions (up and down triangles). Lines correspond to the two parameter description with the combined Arrhenius-Merz law. Panel (b) shows the same data and analysis by plotting against $1/E$. All data taken on sample *SI*. Panel (c) presents a plot of the relaxation times against the scaling argument that is predicted by the combined Arrhenius-Merz law.

temperature only varies by a factor of 2. The large timescales are remarkable as they document the absence of quantum effects in the multiferroic domain inversion. Quantum effects have been observed in tetrathiofulvalene-QBr_2I_2, where one could tune the system resulting in a saturation of the relaxation times upon cooling [37]. In $TbMnO_3$ the objects relevant for the relaxation processes remain classical down to about 13 K. Only close to the multiferroic transition—and above, see Fig. 1(d)—processes become considerably faster compared to the activation extrapolation indicating an intrinsically different mechanism.

When separately fitting the $\log(\tau)$ versus $1/T$ data obtained at a constant electric field, we recognized that these activation fits coincide just at the multiferroic transition temperature, T_{MF}, and a characteristic time τ^*. These individual fits are shown in Fig. S2 in the Supplemental Material [32]. Introducing the constraint $\tau(T_{\mathrm{MF}}) = \tau^*$, the entire dependence of the relaxation times on temperature and electric field can be described by a simple combination of the Merz and the activation Arrhenius law:

$$\tau(E,T) = \tau^* \exp\left[\frac{A_0}{E}\left(\frac{1}{T} - \frac{1}{T_{\mathrm{MF}}}\right)\right] = \tau^* \exp\left(\frac{A_0 T_r}{ET}\right), \qquad (3)$$

with the reduced temperature $T_r = (T_{\mathrm{MF}} - T)/T_{\mathrm{MF}}$. This relation requires only two fit parameters, A_0 and τ^*, to describe the entire data. The results with $A_0 = 1483\ \mathrm{K}\cdot\mathrm{kV/mm}$ and $\tau^* = 0.72$ ms, are shown in Figs. 4(a) and 4(b), which show logarithmic plots of the relaxation times against $1/T$ and $1/E$, respectively.

The relation (3) resembles the empirical behavior $\tau \propto \exp(a_0 \cdot P_s^3/ET)$ [24,25], but the third power of the saturation polarization is not proportional to T_r in a type-II multiferroic. Analyzes of the multiferroic transition in the frame of the Landau theory propose that $P_S \propto T_r^{1/2}$ [38], so that Eq. (3) translates to $\tau \propto \exp(a_0' \cdot P_s^2/ET)$. For ferroelectric lead zirconate titanate films it was proposed that the relaxation times scale with $(1/E)T_r$ [27], while the combined Arrhenius-Merz law in Eq. (3) implies scaling against $(1/E)(T_r/T)$. In Fig. 4(c) we plot the logarithmic relaxation time against this scaling argument $(1/E)(T_r/T)$ obtaining a satisfying scaling. The two scaling concepts are compared in Fig. S6 in the Supplemental Material; clearly the multiferroic data only obey the scaling corresponding with the combined Arrhenius-Merz law.

For the largest part of the E and T ranges studied, the simple relation describes the data very well. This indicates that the rather slow multiferroic relaxation is dominated by a single slow process, which must be the growth of the domains through domain wall motion. Taking into account the topography of the domain structure obtained by second-harmonic-generation mapping [28,29] and the fact that there is no essential change in the neutron-diffraction peak profiles, see [32], the sideways growth is most relevant. The parameter A_0 describes the activation energy generated through domain wall pinning that is proportional to the reduced temperature T_r and to $1/E$. The electric-field dependence just corresponds to the well-established impact of the external field in a ferroelectric material described by the Merz law, while the proportionality to T_r implies that the activation energy follows the square of the polarization, which itself is proportional to the magnetic component condensing at T_{MF} [38]. The characteristic time τ^* denotes the quickest relaxation that can be reached with this formalism and the underlying process, i.e., the domain wall motion. It appears tempting to associate this time with the inverse of the spin-wave velocity, as sound velocities would predict much shorter times and as the very small structural distortions seem inconsistent with structurally dominated domain-wall motion.

Deviations from the combined Arrhenius-Merz law are, however, clearly visible close to the multiferroic transition at high fields, where already the activation fits at fixed electric fields fail, see Fig. S2 in the Supplemental Material [32], and where the stretching exponent increases, see Fig. 3. Close to the transition—and probably also at very high electric fields—the domain inversion becomes faster. We attribute this effect to an additional nucleation that becomes possible close to T_{MF}, because the condensation energies of the multiferroic phase are small. The enhancement of the stretching exponent b close to the multiferroic transition, see Fig. 3(b), also points to additional nucleation processes. In addition, quantum effects can limit the validity of the Arrhenius-Merz relation at low temperature, but the existing data do not indicate such an effect.

The combined Arrhenius-Merz law equally well describes other multiferroics studied by time-resolved polarized neutron diffraction, $Ni_3V_2O_8$, CuO, $(NH_4)FeCl_5{\cdot}H_2O$ [39], and $NaFeGe_2O_6$ [40], underlining the broad applicability of the simple relation. Just $MnWO_4$ exhibits a peculiar temperature dependence of the relaxation times [41], which can be attributed to anharmonic effects associated to its low-temperature commensurate structure [45,46].

In conclusion we have studied the multiferroic domain relaxation in the prototype type-II multiferroic $TbMnO_3$ using polarized neutron diffraction, which permits determining relaxation times over 8 decades. Over a wide range of temperatures and electric fields the domain relaxation can be described by a simple combination of Merz and activation laws with an activation field that is proportional to the reduced temperature, and thus to the square of the electric polarization. The simplicity of this relation indicates that for a wide range of temperatures and fields, multiferroic relaxation is dominated by the slowest process, the domain wall motion. Only close to the multiferroic transition the observed relaxation becomes faster, most likely due to additional nucleation processes.

This work was funded by the Deutsche Forschungsgemeinschaft (DFG, German Research Foundation), Project No. 277146847; CRC 1238 projects A02 and B04; and by the Bundesministerium für Bildung und Forschung, Project No. 05K19PK1. We thank C. Honerlage and E. Lelièvre-Berna for technical support.

*Deceased.
†braden@ph2.uni-koeln.de

[1] H. J. Williams, W. Shockley, and C. Kittel, Studies of the propagation velocity of a ferromagnetic domain boundary, Phys. Rev. **80**, 1090 (1950).
[2] S. Zapperi, P. Cizeau, G. Durin, and H. E. Stanley, Dynamics of a ferromagnetic domain wall: Avalanches, depinning transition, and the Barkhausen effect, Phys. Rev. B **58**, 6353 (1998).
[3] J. F. Scott, *Ferroelectric Memories* (Springer, Heidelberg, 2000).
[4] P. J. Brown, J. B. Forsyth, and F. Tasset, Studies of magnetoelectric crystals using spherical neutron polarimetry, Solid State Sci. **7**, 682 (2005).
[5] P. J. Brown, Spherical neutron polarimetry, in *Neutron Scattering from Magnetic Materials* (Elsevier B. V., New York, 2006), ch. 5, pp. 215–244.
[6] M. Baum, K. Schmalzl, P. Steffens, A. Hiess, L. P. Regnault, M. Meven, P. Becker, L. Bohatý, and M. Braden, Controlling toroidal moments by crossed electric and magnetic fields, Phys. Rev. B **88**, 024414 (2013).
[7] M. Fiebig, D. Fröhlich, S. Leute, and R. Pisarev, Topography of antiferromagnetic domains using second harmonic generation with an external reference, Appl. Phys. B **66**, 265 (1998).
[8] W. Eerenstein, N. D. Mathur, and J. F. Scott, Multiferroic and magnetoelectric materials, Nature (London) **442**, 759 (2006).
[9] T. Kimura, Spiral magnets as magnetoelectrics, Annu. Rev. Mater. Res. **37**, 387 (2007).
[10] D. Khomskii, Classifying multiferroics: Mechanisms and effects, Physics **2**, 20 (2009).
[11] H. Katsura, N. Nagaosa, and A. Balatsky, Spin Current and Magnetoelectric Effect in Noncollinear Magnets, Phys. Rev. Lett. **95**, 057205 (2005).
[12] M. Mostovoy, Ferroelectricity in Spiral Magnets, Phys. Rev. Lett. **96**, 067601 (2006).
[13] Y. Yamasaki, H. Sagayama, T. Goto, M. Matsuura, K. Hirota, T. Arima, and Y. Tokura, Electric Control of Spin Helicity in a Magnetic Ferroelectric, Phys. Rev. Lett. **98**, 147204 (2007).
[14] T. Finger, D. Senff, K. Schmalzl, W. Schmidt, L. P. Regnault, P. Becker, L. Bohatý, and M. Braden, Electric-field control of the chiral magnetism of multiferroic $MnWO_4$ as seen via polarized neutron diffraction, Phys. Rev. B **81**, 054430 (2010).
[15] A. Poole, P. J. Brown, and A. S. Wills, Spherical neutron polarimetry (SNP) study of magneto-electric coupling in the multiferroic $MnWO_4$, J. Phys. Conf. Ser. **145**, 012074 (2009).
[16] A. J. Hearmon, F. Fabrizi, L. C. Chapon, R. D. Johnson, D. Prabhakaran, S. V. Streltsov, P. J. Brown, and P. G. Radaelli, Electric Field Control of the Magnetic Chiralities in Ferroaxial Multiferroic $RbFe(MoO_4)_2$, Phys. Rev. Lett. **108**, 237201 (2012).
[17] J. Stein, M. Baum, S. Holbein, T. Finger, T. Cronert, C. Tölzer, T. Fröhlich, S. Biesenkamp, K. Schmalzl, P. Steffens, C. H. Lee, and M. Braden, Control of Chiral Magnetism Through Electric Fields in Multiferroic Compounds above the Long-Range Multiferroic Transition, Phys. Rev. Lett. **119**, 177201 (2017).
[18] W. J. Merz, Domain formation and domain wall motions in ferroelectric $BaTiO_3$ single crystals, Phys. Rev. **95**, 690 (1954).
[19] Y. Ishibashi and Y. Takagi, Note on ferroelectric domain switching, J. Phys. Soc. Jpn. **31**, 506 (1971).
[20] Y. Ishibashi, Polarization reversal kinetics in ferroelectric liquid crystals, Jpn. J. Appl. Phys. **24**, 126 (1985).

[21] M. Avrami, Kinetics of phase change. I. General theory, J. Chem. Phys. **7**, 1103 (1939).
[22] M. Avrami, Kinetics of phase change. II. Transformation-time relations for random distribution of nuclei, J. Chem. Phys. **8**, 212 (1940).
[23] M. Avrami, Granulation, phase change, and microstructure kinetics of phase change. III, J. Chem. Phys. **9**, 177 (1941).
[24] M. Hayashi, Kinetics of domain wall motion in ferroelectric switching. I. General formulation, J. Phys. Soc. Jpn. **33**, 616 (1972).
[25] M. E. Lines and A. M. Glass, *Principles and Applications of Ferroelectrics and Related Materials* (Oxford University Press, New York, 1977).
[26] H. Orihara and Y. Ishibashi, Switching characteristics of ferroelectric liquid crystal DOBAMBC (II)–temperature dependence and scaling rule–, Jpn. J. Appl. Phys. **24**, 902 (1985).
[27] J. F. Scott, L. Kammerdiner, M. Parris, S. Traynor, V. Ottenbacher, A. Shawabkeh, and W. F. Oliver, Switching kinetics of lead zirconate titanate submicron thin film memories, J. Appl. Phys. **64**, 787 (1988).
[28] D. Meier, N. Leo, M. Maringer, T. Lottermoser, and M. Fiebig, Topology and manipulation of multiferroic hybrid domains in $MnWO_4$, Phys. Rev. B **80**, 224420 (2009).
[29] M. Matsubara, S. Manz, M. Mochizuki, T. Kubacka, A. Iyama, N. Aliouane, T. Kimura, S. L. Johnson, D. Meier, and M. Fiebig, Magnetoelectric domain control in multiferroic $TbMnO_3$, Science **348**, 1112 (2015).
[30] T. Kimura, T. Goto, H. Shintani, K. Ishizaka, T. Arima, and Y. Tokura, Magnetic control of ferroelectric polarization, Nature (London) **426**, 55 (2003).
[31] K. Schmalzl, W. Schmidt, S. Raymond, H. Feilbach, C. Mounier, B. Vettard, and T. Brückel, The upgrade of the cold neutron three-axis spectrometer IN12 at the ILL, Nucl. Instrum. Methods Phys. Res., Sect. A **819**, 89 (2016).
[32] See Supplemental Material at http://link.aps.org/supplemental/10.1103/PhysRevLett.127.097601 for further information on the experimental techniques, additional data on the domain inversion in $TbMnO_3$ as well as a comparison of scaling concepts.
[33] T. Chatterji, *Neutron Scattering from Magnetic Materials*, edited by T. Chatterji (Elsevier B. V., New York, 2006).
[34] G. Eckold, Time-resolved triple-axis spectroscopy–a new method for real-time neutron scattering, Nucl. Instrum. Methods Phys. Res., Sect. A **289**, 221 (1990).
[35] F. Schrettle, P. Lunkenheimer, J. Hemberger, V. Y. Ivanov, A. A. Mukhin, A. M. Balbashov, and A. Loidl, Relaxations as Key to the Magnetocapacitive Effects in the Perovskite Manganites, Phys. Rev. Lett. **102**, 207208 (2009).
[36] An optimized multiferroic material allows one to control the neutron polarization rapidly and opens new perspectives for instrumentation.
[37] F. Kagawa, N. Minami, S. Horiuchi, and Y. Tokura, Athermal domain-wall creep near a ferroelectric quantum critical point, Nat. Commun. **7**, 10675 (2016).
[38] P. Tolédano, Pseudo-proper ferroelectricity and magnetoelectric effects in $TbMnO_3$, Phys. Rev. B **79**, 094416 (2009).
[39] S. Biesenkamp (private communication).
[40] S. Biesenkamp, D. Gorkov, W. Schmidt, K. Schmalzl, Y. Sidis, P. Becker, L. Bohatý, and M. Braden, Chiral order and multiferroic domain relaxation in $NaFeGe_2O_6$, arXiv:2105.06875.
[41] Time-resolved experiments were performed for $MnWO_4$ using second harmonic generation [42], dielectric spectroscopy [43], and neutron diffraction [44]. All studies agree concerning the rather slow time constants of the order of 10 ms. For $MnWO_4$ there is also agreement that the relaxation exhibits a peculiar temperature dependence at constant electric field. Upon cooling in the multiferroic phase, the relaxation first slows but then relaxation times pass a maximum and speed up again towards the low-temperature boundary of the multiferroic phase [43,44].
[42] T. Hoffmann, P. Thielen, P. Becker, L. Bohatý, and M. Fiebig, Time-resolved imaging of magnetoelectric switching in multiferroic $MnWO_4$, Phys. Rev. B **84**, 184404 (2011).
[43] D. Niermann, C. P. Grams, M. Schalenbach, P. Becker, L. Bohatý, J. Stein, M. Braden, and J. Hemberger, Domain dynamics in the multiferroic phase of $MnWO_4$, Phys. Rev. B **89**, 134412 (2014).
[44] M. Baum, J. Leist, T. Finger, K. Schmalzl, A. Hiess, L. P. Regnault, P. Becker, L. Bohatý, G. Eckold, and M. Braden, Kinetics of the multiferroic switching in $MnWO_4$, Phys. Rev. B **89**, 144406 (2014).
[45] S. Holbein, M. Ackermann, L. Chapon, P. Steffens, A. Gukasov, A. Sazonov, O. Breunig, Y. Sanders, P. Becker, L. Bohatý, T. Lorenz, and M. Braden, Strong magnetoelastic coupling at the transition from harmonic to anharmonic order in $NaFe(WO_4)_2$ with $3d^5$ configuration, Phys. Rev. B **94**, 104423 (2016).
[46] S. Biesenkamp, N. Qureshi, Y. Sidis, P. Becker, L. Bohatý, and M. Braden, Structural dimerization in the commensurate magnetic phases of $NaFe(WO_4)_2$ and $MnWO_4$, Phys. Rev. B **102**, 144429 (2020).